Hindawi Publishing Corporation
Journal of Nanomaterials
Volume 2012, Article ID 925750, 11 pages
doi:10.1155/2012/925750

Research Article

Molecular Dynamics Analysis of PVA-*AgnP* Composites by Dielectric Spectroscopy

J. Betzabe González-Campos,[1] Evgen Prokhorov,[2] Isaac C. Sanchez,[3] J. Gabriel Luna-Bárcenas,[2] Alejandro Manzano-Ramírez,[2] Jesús González-Hernández,[4] Yliana López-Castro,[1] and Rosa E. del Río[1]

[1] *Department of Chemistry, Institute of Chemical and Biological Researches, Universidad Michoacana de San Nicolás de Hidalgo, Ciudad Universitaria, 58060 Morelia, MICH, Mexico*
[2] *Biomaterials Laboratory, Centro de Investigación y de Estudios avanzados del IPN, Unidad Querétaro, 76230 Querétaro, QRO, Mexico*
[3] *Department of Chemical Engineering, The University of Texas at Austin, Austin, TX 78712, USA*
[4] *Nanostructurated Materials Laboratory, Centro de Investigación en Materiales Avanzados, S.C., 31109 Chihuahua, CHIH, Mexico*

Correspondence should be addressed to J. Gabriel Luna-Bárcenas, gluna@qro.cinvestav.mx

Received 10 February 2012; Revised 20 May 2012; Accepted 20 May 2012

Academic Editor: Sérgio Henrique Pezzin

The molecular dynamics of PVA/AgnP composites were studied by dielectric spectroscopy (DS) in the 20–300°C temperature range. Improper water elimination leads to misinterpretation of thermal relaxations in PVA composites in agreement with the previous report for pristine PVA. The evaporation of water and its plasticizing effect are more evident in pure PVA confirming the existence of strong interaction between OH groups of PVA chains and AgnP. Dry films show a single nonlinear VFT dependence (from 45°C until melting) associated to the α-relaxation and, therefore, to the glass transition phenomenon and from dielectric measurements, the T_g of composites vary from 88°C for pristine PVA to 125°C for PVA/AgnP (5 wt%). Below 45°C, dry films exhibit a single Arrhenius behavior showing a 3D hopping conductivity as explained based on the variable range hopping model. PVA/AgnP composites have higher conductivity compared to pristine PVA, and it increases as AgnP weight percent increases. Finally, DMA measurements support the statement that a secondary relaxation was erroneously assigned as the glass transition of PVA and composites in previous reports.

1. Introduction

Nowadays metal-polymer nanocomposites are the subject of increased interest because they combine the features of polymers with those of metals. Metallic nanoparticles incorporated in or with polymers have attracted much attention due to their distinct optical, electrical, and catalytic properties, which have potential applications in different fields such as bioengineering, photonics, and electronics [1–5]. Among different metals used for nanoparticles preparation, silver is very attractive because it exhibits the highest electrical and thermal conductivities, together with their antibacterial activity and even their interaction with HIV-1 virus [6]. On the other hand, polyvinyl alcohol (PVA) has been widely used as a matrix for preparation of nanocomposites due to its easy processability and high optical clarity. It is considered among the best polymers as host matrix for silver nanoparticles (AgnP), and it is frequently used as a stabilizer due to its optical clarity, which enables investigation of the nanoparticle formation [7, 8]. PVA is a biologically friendly polymer since it is water soluble and has extremely low cytotoxicity, which allows the application of PVA-based composites in the biomedical field.

PVA/AgnP is a very attractive combination since these composites have high mechanical strength, water-solubility, good environmental stability, easy processability, and electrical conductivity [9–11]. Different studies have been carried out about the optimal parameters for the synthesis of nanoparticles, the antibacterial activity of composites, their mechanical properties, and the chemical interaction between

PVA and AgnP [12–15]. However, the molecular dynamics analysis by dielectric relaxation studies and the electrical conductivity behavior of PVA-Ag nanocomposite films have been scarcely studied; there is only one report in this regard [16].

One parameter that can be characterized by means of the molecular dynamics analysis is the glass transition temperature (T_g). In polymers, polymers blends, and composites, an accurate characterization of the T_g plays a crucial role, since it indicates the change from the glassy state into a liquid or a rubbery state, and it can be a measure of compatibility or miscibility in polymer blends [17]. Additionally, physicochemical properties of a material such as dissolution, bioavailability, processing, and handling qualities can be related to the glass transition temperature of the material [18]. Also the optimal application and processing temperatures for polymers base materials are dependent on their glass transition temperature.

On the other hand, in a previous work [19], it was shown by dielectric and dynamic mechanical analysis that the nature of pure PVA thermal relaxations was erroneously assigned, since improper water elimination and the narrow temperature range analyzed in all the previous reports have led to misinterpretation of thermal relaxations in pure PVA. Commonly, the molecular dynamics analysis of PVA composites, and its blends with other polymers and inorganic compounds has been carried out in a narrow temperature range and based on pure PVA thermal relaxations behavior; however, if the molecular dynamics of pure PVA has been misunderstood, it could also be the case of the molecular dynamics of its composites and blends.

Based on these arguments, the aim of this work is twofold: to study the molecular dynamics of PVA/AgnP composites, which have been scarcely reported, and to make a comparison based on the previous studies on pure PVA to probe that previous reports on PVA-inorganic materials composites have also been misunderstanding because they were based in pure PVA results.

2. Experimental Methods

2.1. Films Preparation. Poly(vinyl alcohol), Mw 89,000–98,000 g/mol and hydrolysis degree >99%, was purchased from Sigma-Aldrich and used as received. Carbon-coated silver nanoparticles powder 25 nm average particle size was purchased from nanotechnologies, Inc. PVA films were obtained by dissolving a known amount of PVA in water to obtain a 7.8 wt % solution under stirring at 90°C. The proper quantity of silver nanoparticles powder (0.5, 1, 2, 3 and 5% w/w respect to PVA dry based) was poured into the 7.8 wt % aqueous PVA solution, this solution was mechanically stirrer for 40 min and further sonicated during 30 min to obtain a homogeneous nanoparticle solution. Afterward PVA/AgnP films were prepared by the solvent casting method, by pouring the solutions into plastic Petri dishes and allowing the solvent to evaporate at 37°C during 24 hours. These films had thicknesses of ca. 40 μm measured by a Mitutoyo micrometer. A thin layer of gold was vacuum-deposited onto both film sides to serve as electrodes. Rectangular small pieces (about 4 mm × 3 mm) of these films were prepared for measurements, and the contact areas were measured with a digital calibrator (Mitutoyo).

2.2. Infrared Measurements and Morphology Analysis. Chemical analysis of PVA/AgnP composites was performed by FTIR on a Perkin-Elmer spectrophotometer using an ATR accessory in the range 4000–650 cm^{-1}. Resolution was set to 4 cm^{-1}, and the spectra are an average of 32 scans. PVA/AgnP films morphology was analyzed by JEOM JSM-7401F field emission scanning electron microscope.

2.3. Thermal Measurements. Moisture content was determined by thermogravimetric analysis (TGA). The moisture content was evaluated by the decrease of sample weight during the heating scan. TGA curves were obtained using a Mettler Toledo apparatus, model TGA/SDTA 851e, with a sample mass of ca. 3 mg and an aluminum sample holder under argon atmosphere with a flow rate of 75 mL/min. Heating rate was set to 10°C/min.

2.4. Dielectric Measurements. The dielectric measurements in the frequency range from 0.1 Hz to 1 MHz were carried out using a Solartron 1260 impedance gain-phase analyzer with 1294 Impedance interface and in the frequency range 100 Hz–110 MHz using an Agilent Precision Impedance Analyzer 4294A. The amplitude of the measuring signal was 100 mV. The home-made impedance vacuum cell was used in conjunction with a Watlow's Series 982 microprocessor with ramping temperature controller for all dielectric measurements from 20°C to 300°C, and for some samples with an additional thermal treatment at 120°C to obtain "dry" samples. Each sample was left at each temperature for 3 min to ensure thermal equilibrium.

2.5. Dynamic Mechanical Analysis (DMA). DMA measurements were carried out using an RSAIII, TA Instruments with a heating rate of 5°C/min at a frequency of 0.1 Hz, under dry air atmosphere in the 25–300°C temperature range.

3. Results and Discussion

3.1. Morphological Analysis. The AgnP dispersion on PVA matrix analyzed by SEM is shown in Figure 1. At lower concentration, a homogeneous dispersion of AgnP is observed since they are well distributed within the PVA matrix with particles size of 25 nm. When AgnP concentration increases, the formation of agglomerates cannot be avoided; however, the dispersion of silver nanoparticles is adequate and clusters are not significant. Uniform metal nanoparticles dispersion is required to guarantee the homogeneity on properties. The used methodology gives well dispersed films even at high concentration such as 5% wt.

It could be seen that PVA is an excellent host matrix for encapsulation of silver nanoparticles acting as a good capping agent and providing environmental and chemical stability.

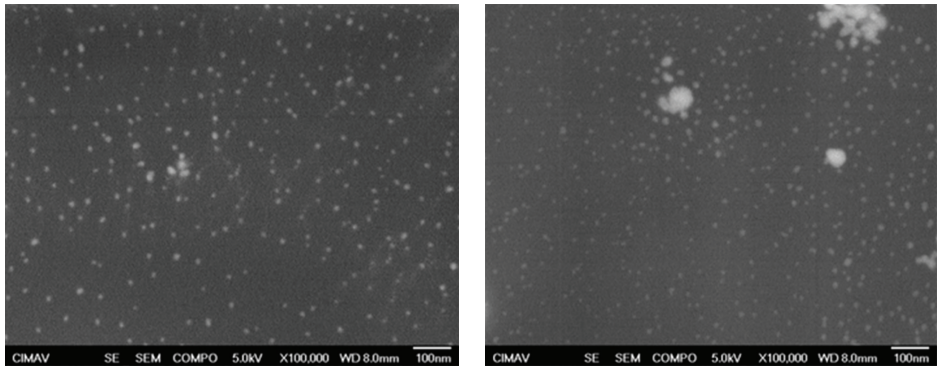

(a) (b)

Figure 1: (a) PVA/AgnP (2%) and (b) PVA/AgnP (5%) films.

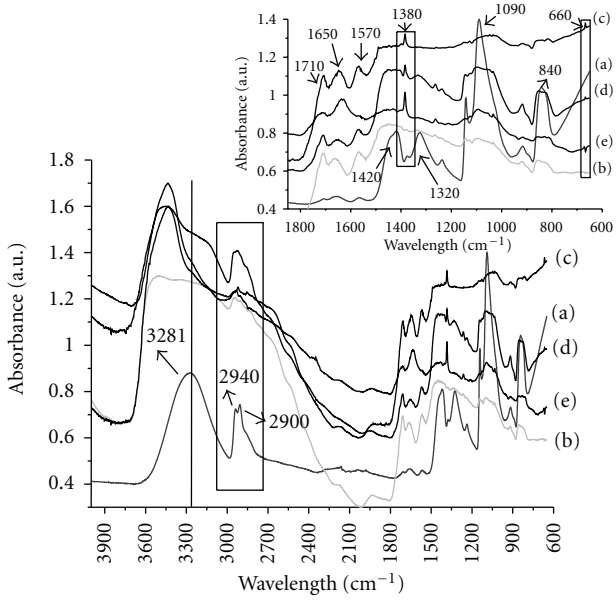

Figure 2: IR spectra of pristine PVA and PVA/AgnP composites. Window insert: zoom for the 1800 cm^{-1} to 600 cm^{-1} region.

3.2. FTIR-ATR Analysis. The FTIR spectra for pristine PVA and PV/AgnP composites are shown in Figure 2. The spectrum of pristine PVA shows its characteristic bands at 1040 cm^{-1} (C–O) in acetyl group, 1090 cm^{-1} (C–O), 1140 cm^{-1} (C–O, crystallinity), 1170 cm^{-1} (C–O–C) in ether group, 1245 cm^{-1} (C–O–C) in acetyl group, 1320 cm^{-1} (CH + OH interaction), the 1375 cm^{-1} band due to the coupling of O–H vibrations at 1420 cm^{-1} with the wagging vibrations (CH_2), 1650 cm^{-1} (C=C), 1730 cm^{-1} (C=O), 2850 cm^{-1} (CH), 2900–2950 cm^{-1} (CH_2), and 3000–3500 cm^{-1} (O–H).

Figure 2 also shows clear evidence of chemical interactions bonding between PVA and silver nanoparticles suggesting that these interactions are mainly between –OH groups of PVA and AgnP. This is observed by a general change in the intensity of the absorption bands in the stretching vibrations of OH groups involved in hydrogen bonding (3800–3000 cm^{-1}) and their shifting to 3400 cm^{-1}. The PVA-AgnP's spectrums show a new band at 660 cm^{-1} corroborating the formation of hydrogen bonds in all structures. A change in the intensity of the band at 1380 cm^{-1}, compared with the band at 1420 cm^{-1}, indicates the decoupling between OH and CH vibrations due to bonding interaction between OH and silver nanoparticles.

3.3. Moisture Content. For pristine PVA as well as for PVA/AgnP composites, two different moisture contents according to different sample treatment were evaluated: wet samples (without annealing treatment) and annealed samples at 120°C. Samples annealed at 120°C were obtained by the following fashion: a first scan was performed from 20°C to 120°C holding them at 120°C during 30 minutes and followed by cooling at 20°C, afterward a second heating from 20°C to 250°C was carried out in the same sample. Before annealing, a single scan on wet samples was performed for comparison. In the case of dry films, water content is reduced to the minimum possible by the heat treatment at 120°C during 30 minutes under controlled atmosphere inside the measuring cell.

Thermogravimetric measurements for pristine PVA are shown in Figure 3. The curve labeled as "wet PVA" corresponds to the first scan described above (from 20 to 120°C), while that labeled as "dry PVA" is the second scan of the same film after heat treatment at 120°C during 30 minutes. The water loss is about 4.16% and 0.01% for wet and dry samples, respectively; these results show that an important quantity of water is present before any measurement of PVA films. It is noteworthy that water content in PVA/AgnP composites is very close to that reported for pristine PVA; however, it slightly decreases as AgnP increases (from 4.0% for 0.05% of AgnP to 3.6% for 5% of AgnP). For all samples studied, the second scan after annealing at 120°C (dry samples) reveals water loss about 0.01%; therefore, samples annealed at 120°C do not need further heating treatment since at this water content, it is considered that samples are in the dry state.

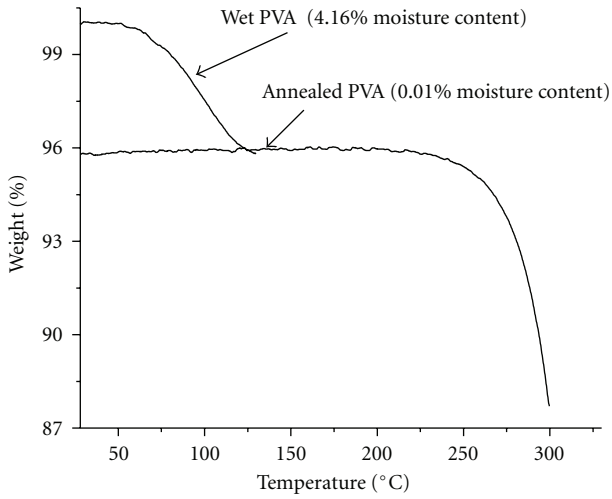

Figure 3: Thermogravimetric measurements in pristine PVA.

These same conditions labeled as wet and dry samples were applied in dielectric and DMA measurements discussed below.

3.4. Conductivity and Dielectric Results. The dc conductivity (σ_{dc}) of PVA and PVA/AgnP films was calculated by dielectric measurements using the methodology previously described elsewhere [20–22]. The dc resistance (R_{dc}) was obtained from the intersection of the semicircle and the real-part axis on the impedance plane (at $Z'' = 0$) as it is pointed out in the window insert of Figure 4, hence σ_{dc} can be calculated by the following relationship: $\sigma_{dc} = d/(R_{dc} \times A)$, where d are the thickness and A the area of the film, respectively. The Cole-Cole plot (real (Z') versus imaginary (Z'') parts of the impedance) shows the high frequency region semicircle, which is related to the bulk effect of PVA composites, while the linear region in the low frequency range is attributed to contacts effect [20].

As showed by TGA analysis, at ambient conditions water content in films is ca. 4.16 wt%, which reduces film resistance and masks the real conductivity behavior of composites. This is a delicate issue that needs to be considered when performing dielectric measurements especially in PVA films [19]. Due to this observation, dielectric measurements were carried out on dry films annealed in vacuum cell.

Figure 4 shows the change in dc conductivity as a function of temperature from 25 to 250°C for PVA and PVA/AgnP (0.5 and 1%) wet films. It can be seen in both films that conductivity increases as temperature increases due to the increased free volume and their respective ionic and segmental mobility [23]. This dependence unveils two well-defined regions at "low" (from 20°C to 80°C) and high (from 100°C to melting) temperatures, with an intermediate discontinuity between 80°C and 100°C associated to moisture evaporation [19]. Both relaxation regions disclose a well-defined non-Arrhenius behavior usually observed in many glass-formers and well described by the well-known Vogel-Fulcher-Tammann (VFT) relationship:

$$\sigma_{dc} = \sigma_0 e^{[-D/(T-T_0)]}, \quad (1)$$

where σ_{dc}, σ_0, and D are the conductivity, the preexponential factor, and a material constant, respectively, and T_0 is the so-called Vogel temperature related to the glass transition temperature [20]. This VFT-behavior is a clear evidence for the glass transition phenomenon; however, at this point this trend is not disclosed in the whole temperature range as in many amorphous polymers such as polypeptides [24]. At this point, it would be ambiguous to assign a T_g value of plasticized PVA and composites even though the plasticization of T_g is evident, the evaporation of water could be interfering.

Previously, these two regions were erroneously described as two Arrhenius-type relaxations in pristine PVA and Gd doped-PVA [25]; however, in those composites, moisture was not properly eliminated and the analysis was performed in a narrow temperature range (from 30°C to 180°C for composites and from 30°C to 160°C for pristine PVA), this do not allow to have a wider panorama of PVA and Gd doped-PVA relaxations giving rise to the erroneous interpretation. It is also important to mention that Hanafy did not discuss the evaporation of water zone (indicated in Figure 4), even when it is clearly observed in the ac conductivity versus the reciprocal temperature plot for PVA and Gd doped-PVA (see [25]).

From Figure 4, it is noteworthy that the evaporation of water (about 80°C–100°C) is more evident in pure PVA. This event confirms the existence of strong interactions between water and pristine PVA chains, and it clearly indicates the existence of strong hydrophilic groups acting as primary hydration sites: OH side groups. In pristine PVA, an overall increase in the molecular mobility with increasing water content occurs. This water evaporation region arises as a consequence of loosely bound water molecules connected to the reorientation of water molecules in water clusters around the primary hydration sites. The hydroxyl groups exert strong effects on the PVA molecular dynamics since the interactions between OH neighbors and absorbed moisture. The evaporation of water is less evident in PVA/AgnP composites; the conductivity slightly changes in the 80°C–100°C region, but it also represents a transition region from the low temperature relaxation to the high temperature relaxation.

As it was pointed out by IR analysis, the Ag nanoparticles directly interact with OH groups in PVA chains. This interaction decreases the number of PVA-water hydrogen bonds, reducing the number of available OH primary hydration sites to attach water molecules and consequently decreasing the moisture content. Since less amount of water is present in PVA/AgnP composites, the evaporation of water region is less evident. An additionally VFT-low temperature relaxation (between 20°C and 80°C) in all PVA/AgnP wet samples shows lesser curvature, thus indicating that the plasticizing effect of water is less effective.

On the other hand, wet PVA/AgnP composites have higher conductivity compared with pristine PVA, and it

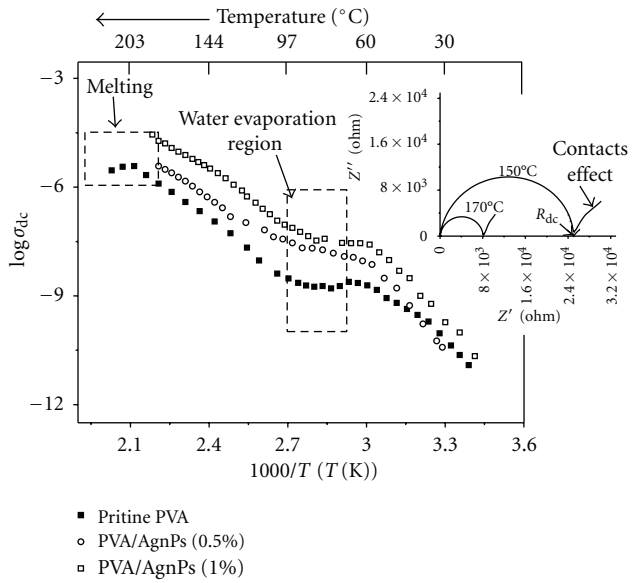

FIGURE 4: Conductivity (σ_{dc}) versus *1000/T*(K) for pure PVA and PVA/AgnP wet composites.

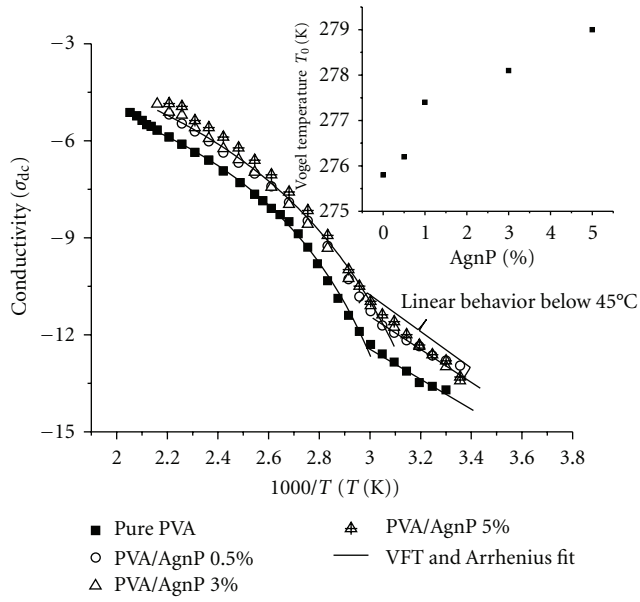

FIGURE 5: DC conductivity versus *1000/T*(K) for dry PVA/AgnP films (water content near zero). Window insert: Vogel Temperature *versus* AgnP % wt.

increases as AgnP weight percent increases as it can be seen in Figure 4. The formation of charge transfer complexes (CTCs) by the inclusion of metal nanoparticles cause reduction of the crystalline-amorphous interface decreasing the interfacial barrier and increasing the transition probability of electron hopping across the barrier and insulator chains, which in turn provides a conducting path through the amorphous regions of the polymer matrix resulting in enhanced conductivity in agreement with Mahendia et al. [16].

At the same time, the melting temperature of PVA is affected by the inclusion of AgnP; in PVA/AgnP composites, the melting temperature shifts to lower values. This can be explained as follows: the crystallinity of PVA results from strong intermolecular and intramolecular hydrogen bonding between PVA chains mainlythrough –OH groups. As it was shown by FTIR measurements, AgnP interactwith –OH groups of PVA; therefore, these AgnP-OH interactions decrease the intermolecular hydrogen bonding in PVA chains affecting its crystallinity, which in turns directly affects the melting temperature. This observation has been previously studied by our group [19].

On the other hand, based on previous studies on pure PVA [19], dry films of PVA/AgnP composites were obtained; in this case, water content is reduced to the minimum possible by a thermal treatment at 120°C during 30 minutes under controlled atmosphere inside the measuring cell (water content ca. 0.01%, determined by TGA analysis). After this thermal treatment, the films are cooled down at room temperature without opening the measuring cell, and a second heating is carried out on the same films. Now the conductivity behavior of PVA/AgnP composites is similar to the results previously reported on pristine dry PVA [19], disclosing a different trend compared with wet films, as it can be seen in Figure 5.

The second conductivity scan of dry films shows a single nonlinear VFT dependence from 45°C until melting, preceded by a linear behavior associated to a secondary relaxation process. This linear behavior will be discussed later.

The nonlinear behavior clearly described the glass transition phenomenon in PVA and PVA composites, thus, a single Vogel temperature can be now calculated from the fitting of the experimental data to the VFT model. This results support the statement about the plasticizing effect of water in the 20°C–80°C region and the evaporating of water region in the 80°C–100°C temperature range previously described.

Figure 5 reveals that when PVA/AgnP composites are analyzed in a broad temperature range, it is possible to observe a wider panorama on the true nature of the relaxation processes in PVA and PVA composites. In general, all reported studies on PVA composites and blends were reported up to 180°C.

As mentioned before, there is only one report on PVA-AgnP dielectric measurements [16]; however, it presents conductivity and dielectric studies as a function of AgnP concentration with no temperature variation; there are no previous reports on conductivity and dielectric measurements temperature dependencies regarding PVA-AgnP composites. Nonetheless, several dielectric studies were performed on PVA and PVA composites; however, most of them were carried out below 110°C [16, 23, 25–29]. In these studies, both VFT and Arrhenius behaviors have been reported in pure PVA and its composites in the same narrow temperature range.

Agrawal and Awadhia [26] and Linares et al. [27] showed the VFT behavior for the temperature dependence of conductivity in pure PVA and PVA-based gel electrolytes

Table 1: Vogel and glass transition temperatures for different AgnP content.

Sample	T_0 (K)	T_g (°C)
Pristine PVA	275.8	72.65
PVA/AgnP (0.5 wt%)	276.8	73.15
PVA/AgnP (1 wt%)	277.5	74.35
PVA/AgnP (3 wt%)	278.1	74.95
PVA/AgnP (5 wt%)	279.0	75.85

in the 20–100°C temperature range, and in pure PVA and in PVDF/PVA blends in the 20–110°C temperature range respectively. On the other hand, Hanafy [25] reported two linear behaviors in the 20°C to 180°C temperature range for PVA and Gd-doped PVA. Bhargav et al. [23] suggest an Arrhenius behavior in pure PVA and PVA:NaI complex in the 20–100°C temperature range, as well as Hema et al. [28] in the 20–70°C temperature range in pure PVA and PVA-NH4Br complexes. Zhang et al. [29] showed the relaxation time temperature dependence of PVA/MWCNT composites with 3 wt% MWCNT suggesting an Arrhenius-type dependence in the 20°C to 145°C temperature range. In the latter case, no results for pure PVA are reported. Finally, Mahendia et al. [16] carried out electrical conductivity and dielectric spectroscopy studies of PVA-Ag nanocomposite films; they observed a strong influence of the concentration of silver nanoparticles on the electrical conductivity and dielectric properties of PVA matrix. However, these results are at room temperature and they do not show temperature dependencies of conductivity and dielectric results. Despite of all the above studies, one cannot conclude the existence of a non-Arrhenius, α-relaxation process.

The nature of the molecular dynamics of Arrhenius-type and VFT-type behaviors is very different; it is very important to establish which of them is truly present in a polymer system. Arrhenius-type relaxation is related to the ions that are decoupled from the polymer host, and activated hopping is required for ionic transport. VFT behavior describes the cooperative motion, which occurs when the system is in the vicinity of a glass-transition.

In the case of PVA and PVA composites, VFT behavior was not observed in a number of previous studies on PVA composites because the effect of water was not properly taken into account [23, 25, 28, 29]. The relaxation analysis on those studies was based on temperature ranges not exceeding 160°C; most of them were done up to 100°C. These two factors, moisture and temperature range, are extremely important to gain a better understanding of PVA composites molecular dynamics.

In this work, it is clearly observed that a wider temperature range (in this case from 20°C to 250°C) and an adequate moisture content elimination allow to disclose the true nature of the molecular dynamics in PVA and PVA composites; in this case, the VFT behavior related to the glass transition.

The Vogel temperature (T_0) calculated from de VFT relationship (1) as a function of AgnP content for PVA/AgnP composites is plotted in the window insert of Figure 5 and

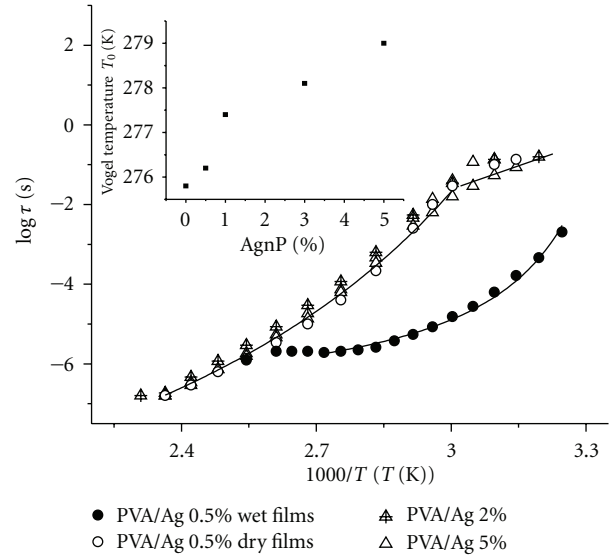

Figure 6: Relaxation time (τ) versus *1000/T (T in* K*)*.

it is shown in Table 1. In general, it can be observed that T_0 increases as AgnP content increases. For most polymers, the relationship between the glass transition temperature T_g and T_0 is $T_g = T_0 + C$, where C is an empirical constant. In many dielectric studies, C is taken as 70 K [30–32]. Table 1 shows the estimated T_g values for pristine PVA and PVA/AgnP composite as a function of AgnP content (C value is taken as 70 K).

Therefore, we can say that the glass transition temperature of PVA composites increases as AgnP weight percent increases in contrast with previous results in Ag-PVA films [33]. Moisture content of PVA composites is lower than that of pristine PVA due to the interaction between OH groups and AgnP; higher glass transition temperature values for PVA composites are expected. AgnP bonds to hydroxyl groups reduce the plasticizer effect and complicate molecular motion in PVA chains resulting in an increase in T_g values.

On the other hand, it has recently been recognized that contact and interfacial polarizations are to account when analyzing dielectric spectra. Indeed, it is well known that dc conductivity strongly affects the loss factor ε'' in the low-frequency range, and a correction must be applied to unmask the polymer dielectric effects [20]. dc Conductivity and contact polarization effect could mask the real dielectric relaxation processes in the low frequency range; therefore, to analyze the dielectric processes in detail, the complex permittivity ε^* is converted to the complex dielectric modulus M^* by the following equation: $M^* = 1/\varepsilon^* = M' + iM'' = [\varepsilon'/(\varepsilon'^2+\varepsilon''^2)+\mathbf{i}\ \varepsilon''/(\varepsilon'^2+\varepsilon''^2)]$, where M' and M'' are the real and imaginary parts of electric modulus and ε' and ε'' are the real and imaginary part of permittivity, respectively. The dielectric modulus is commonly used to analyze dielectric experimental data because interfacial polarization, electrode contribution, and conductivity dc effect do not affect M'' peak. Note that M'' is temperature dependent [34].

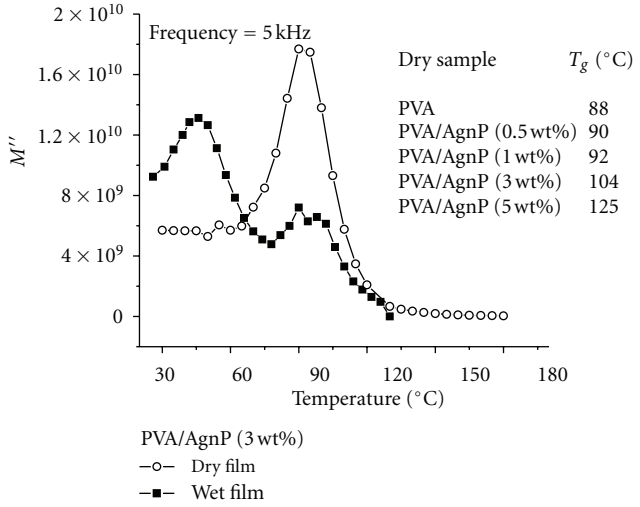

Figure 7: Imaginary part (M'') of the dielectric modulus (M^*) versus Temperature (°C) for PVA/AgnP (3%wt) wet and dry films.

The relaxation time dependence on temperature shown in Figure 6 was obtained from the maximum of the imaginary part of the dielectric modulus (M^*), with the M'' peak ($\tau = 1/2\pi f_{\max}$) calculated at each temperature. The wet films display the trend akin to conductivity as temperature increases: two VFT behaviors in the high and low temperature range separated by moisture evaporation effect in the 80°C to 100°C temperature range. The T_0 calculated from the VFT model for relaxation time: $\tau_{dc} = \tau_0 e^{[D/(T-T_0)]}$ (where τ, τ_0, and D are the relaxation time, the preexponential factor, and a material constant, respectively, and T_0 is the so called Vogel temperature) for all composites are shown in window insert of Figure 6. In dry films, once again the Vogel temperature increases as AgnP concentration increases and relaxation times increase as AgnP concentration increases, and these values are in agreement with those calculated above by the conductivity plot. The interaction of AgnP with OH groups hinders the mobility of PVA chains resulting in higher relaxation times for this primary relaxation.

The α-relaxation process is strongly dependent on moisture content since for the conductivity dependence on temperature, the relaxation time dependence for dry films is very different than that for wet films. After annealing, two well-defined behaviors are observed. A nonlinear behavior from 45°C to melting related to the α-relaxation process, and below 45°C an Arrhenius behavior associated to a secondary relaxation process which will be discussed later.

The results suggest a plasticizing effect of water on PVA composites in agreement with the results previously reported for pristine PVA [19]. A plasticized T_g can be observed in wet films through a nonlinear behavior described by the VFT model separated by the water evaporation region from a second nonlinear behavior disclosed at higher temperature. However, once water is eliminated by thermal treatment, this plasticized T_g vanished and only one nonlinear behavior is observed from 45°C to melting. Also the relaxation time for wet films is lower since the segmental motion is favored by water, by increasing the free volume between chains and because the orientation polarization of polar molecules is slowed down. However, this plasticizing effect is less evident in PVA composites when compared to pristine PVAwith their water content being lower.

More information about moisture effect is provided by means of the complex modulus M^*, specifically by the M'' versus *Temperature* plot for wet and dry PVA and PVA composites as it is shown in Figure 7. In wet samples, two relaxations peaks (one below 50°C and another one above 80°C) at 5 kHz were found. As frequency increases, both peaks shift towards higher temperatures. These two relaxation peaks have been previously reported by other authors from M'', ε'', and tan δ plots for pure PVA, PVA blends, and composites [23, 25, 32–34]. These relaxations were previously assigned as the β-relaxation ascribed to side-group dipoles orientation (relaxation below 80°C, T_β = 40°C for pristine PVA [not shown] and 46°C for PVA/AgnP composite) and the glass transition of PVA (ca. T_g = 85°C), respectively [23, 25, 27, 35, 36]. Nonetheless, our results show that for dry samples the lower temperature relaxation peak (below 50°C) vanishes after annealing the films at 120°C, remaining the α-relaxation peak at the same temperature for each frequency. This fact leads to the conclusion that the low temperature relaxation in wet samples can be traced to a moisture effect, and it does not correspond to a local mode β-relaxation. In this study, for pristine PVA dry samples T_g is ca. 88°C in agreement with previous results [19]. From Figure 7, it can also be observed that T_g increases with AgnP content; for PVA with AgnP 3 wt%, T_g is ca. 92°C. T_g values of composites and pristine PVA, calculated from the dielectric modulus plots as a function of AgnP content in dry films, are shown in Figure 7. It could be observed, that these T_g values are very different from those calculated by the empirical rule. Based upon our previous studies on pristine PVA [19] and chitin and chitosan nanocomposites [20–23], we propose to use the T_g analysis based upon the modulus rather than the use of the empirical rule.

PVA and moisture interaction would correspond to the formation of hydrogen bonds between PVA hydroxyl groups and water, and hydrogen bonds are the dominant interaction responsible for the structure as well as its molecular dynamics. It is possible that the interaction between OH groups and moisture is capable to destroy inter- and intrachain bonding in PVA affecting its crystalline regions; therefore, water acts as a plasticizer by an increase of the free volume in the amorphous phase [37]. This OH groups moisture interaction is disturbed by AgnP inclusion, and as a consequence, the molecular dynamics of both relaxation processes is strongly affected. The low temperature relaxation shifts to higher temperature as AgnP content increases resulting from lower moisture content and lower mobility.

On the other hand, regarding the behavior disclosed in dry films below 45°C previously observed in Figures 5 and 6 (conductivity and relaxation time dependences), it could be seen that this relaxation follows a single Arrhenius behavior, which corresponds to a secondary relaxation process. In glassy polymers, the chains are frozen and molecular motions involved in secondary relaxations occur at higher time

scale (i.e., higher relaxation times) as it is observed in Figure 6. This linear dependence can be explained based on the variable range hopping model. For most polymers this dependence of the dc Conductivity on temperature (T) is often represented by the variable range hopping (VRH) model proposed by Mott [38, 39]:

$$\sigma_{\mathrm{dc}}(T) = \sigma_0 \exp\left[-\left(\frac{T_0}{T}\right)^{\gamma}\right], \quad (2)$$

where σ_0 can be considered as the limiting value of conductivity at infinite temperature and $\sigma_0 \sim 1/T^{1/2}$ [40], T_0 depends on the localization and density of the states, and the exponent γ is related to the dimensionality d of the transport process via the equation $\gamma = 1/(1+d)$, where $d = 1, 2, 3$. The applicability of the VRH model is examined by plotting the experimental results in the form of $\log \sigma(T)^{1/2}$ versus $T^{-\gamma}$ [39].

The experimental data in the 0°C to 45°C temperature range plotted according to the VRH model are presented on Figure 8. It is noteworthy that the dependence $\log \sigma(T)^{1/2}$ versus $T^{-\gamma}$ can be linearly fitted with both $\gamma = 1/4$ and 1/3. However, the best least-square fitting is obtained for $\gamma = 1/4$ (with $R^2 = 0.994$). This value corresponds to a three-dimensional transport process as explained before.

Furthermore, Linares et al. [28] reported the same linear behavior below 21°C for PVDF/PVA blends with different weight percent ratios. They ascribed this low temperature relaxation to a subglass relaxation process occurring in the amorphous phase and associated it to the polar groups attached to the polymeric chain. However, in our case, the application of the variable range hopping model is more appropriate to describe the AgnP-PVA system, since the inclusion of metal nanoparticles give rise to the formation of charge transfer complexes (CTCs) causing the reduction of the crystalline-amorphous interface, decreasing the interfacial barrier and increasing the transition probability of electron hopping across the barrier and insulator chains, which in turn provides a conducting path through the amorphous regions of the polymer matrix resulting in enhanced conductivity [16].

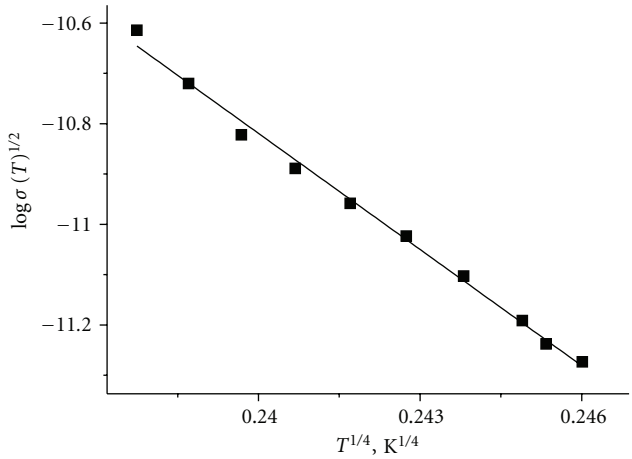

Figure 8: $\log \sigma T^{1/2}$ versus $T^{1/4}$ for pure PVA.

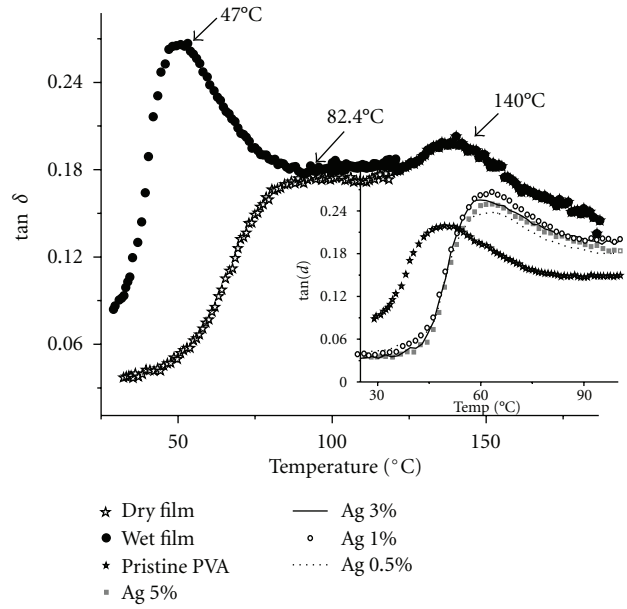

Figure 9: tan δ versus temperature for dry and wet pristine PVA film. Window insert: tan δ versus temperature for wet pristine PVA and wet PVA/AgnP composites.

3.5. Dynamic Mechanical Analysis (DMA). Gautam and Ram [33] report the preparation and thermomechanical properties of Ag-PVA nanocomposites; however, they do not discuss the strong influence of water content on the composite's relaxation processes. In the mentioned study, it is evident that authors assigned the glass transition temperature of PVA/AgnP composites dismissing the effect of water on the relaxation process of composites since the reported values are below 40°C which correspond to the plasticized T_g.

DMA analysis performed at 1 Hz in pristine PVA, and its composites wet and dry films are shown in Figure 9. All samples showed similar behaviors before and after being annealed. It can be observed that the tan δ peak in wet films shows a relaxation process near 40°C. This low temperature DMA peak was previously assigned several times as the glass transition temperature of pristine PVA and several PVA composites. Gautam and Ram [33] assigned T_g values between 40°C and 36°C in Ag-PVA nanocomposites depending upon Ag content. Tian and Tagaya [41] observed this peak around 50°C and described it as the glass transition of pristine PVA. They also show peaks for perlite/PVA and OMMT/PVA nanocomposites without taking into account water content. Yang et al. [42] assigned 44°C and 45°C values for the glass transition temperatures of pristine PVA and PVA/10 wt% montmorillonite (MMT) composites, respectively. They discussed that the T_g values from the DMA analyses for polymer membranes were lower than those from the DSC analyses (71–82°C) because the sensitivity for the measurement of a glass transition temperature by DMA is more sensitive than that by DSC.

However, it is noteworthy that this tan δ peak vanishes in dry films after annealing at 120°C; consequently, this peak

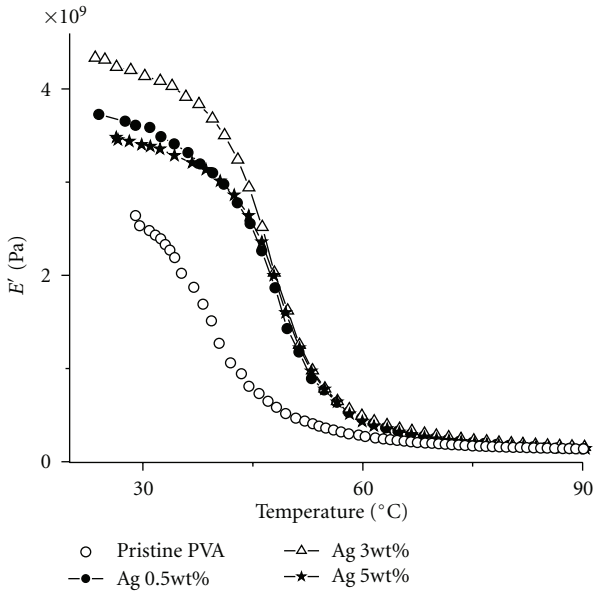

Figure 10: DMA storage modulus (E') versus temperature for wet pristine PVA and wet PVA/AgnP composites.

is related to water-polymer motions which mask the glass transition in wet films. After water evaporation, dry films disclose the glass transition event above 80°C.

Window insert of Figure 9 shows the variation of tan δ peak in wet PVA and PVA/AgnP composites films (water content around 4.1% calculated by TGA). Once again the influence of AgnP on PVA moisture absorption capacity is observed, that is, water-polymer motion is restricted by the presence of silver nanoparticles, which reduces moisture content in composites shifting the relaxation process from 47°C for pristine PVA to 63.8°C for the higher concentration of AgnP (5 wt%).

The storage modulus is shown in Figure 10, it can be seen that it increases as AgnP content in films increases up to 3 wt% suggesting significant reinforcement effect of Ag nanoparticles. Nanoparticles restrict the polymer's chain mobility due to their large surface area and their van der Waals attraction to the polymer matrix, causing the strengthening of mechanical properties of nanocomposite films [33]. However, at 5 wt% of AgnP, the storage modulus decreases compared to lower concentrations, but it remains higher than pristine PVA.

Gautam and Ram [33] showed this reinforcement up to 0.2 wt% of AgnP and then decreases for higher concentrations, being even lower than that of pristine PVA at concentration above 1 wt%. This decrease in the storage modulus is ascribed to the formation of large agglomerates, which in turns affects moisture content of PVA. The interaction between OH groups of PVA and moisture affects the crystalline regions. This OH groups moisture interaction is disturbed by AgnP inclusion resulting in lower moisture content and lower mobility; thus the strengthening of AgnP is less effective at higher concentrations of nanoparticles.

4. Concluding Remarks

The molecular dynamics of PVA/AgnP composites was studied by impedance spectroscopy in the 0.1 Hz to 110 MHz and 20°C to 300°C frequency and temperature ranges, respectively. As well as for pristine PVA, improper water elimination analysis in PVA composites could lead to misinterpretation of thermal relaxations in PVA composites such that a plasticized T_g for wet films has been assigned as a secondary β-relaxation in a number of previous studies in the literature.

Two well-defined nonlinear regions at low and high temperatures, with an intermediate discontinuity between 80°C and 100°C associated to moisture evaporation, were observed in wet PVA/AgnP composites films in agreement with pristine PVA behavior. Previously, these two regions were erroneously assigned to two Arrhenius-type relaxations in pristine and doped PVA. The evaporation of water and its plasticizing effect are more evident in pure PVA confirming the existence of strong interaction between OH groups of PVA chains and AgnP, as shown by FTIR analysis. Dry films show a single nonlinear VFT dependence (from 45°C until melting) associated to the α-relaxation and, therefore, to the glass transition phenomenon. T_g of composites increases as AgnP content increases from 88°C for pristine PVA to 125°C for PVA/AgnP (5 wt%). Below 45°C, dry films exhibit a single Arrhenius behavior showing a 3D hopping conductivity as explained based on the variable range hopping model.

PVA/AgnP composites have higher conductivity compared to pristine PVA, and it increases as AgnP weight percent increases. The inclusion of metal nanoparticles decreases the interfacial barrier and increases the transition probability of electron hopping across the barrier and insulator chains, which in turn provides a conducting path through the amorphous regions of the polymer matrix resulting in enhanced conductivity.

Finally, DMA measurements support the statement that a secondary relaxation was erroneously assigned as the glass transition of PVA and composites in previous reports.

Acknowledgments

The authors thank José Alfredo Muñoz, Araceli Mauricio, and María del Carmen Díaz for their help provided. They also thank CONACYT (Mexican Government) for partial financial support. The authors are not partially or fully associated with Nanotechnologies nor do they endorse the use of their products.

References

[1] A. Henglein, "Small-particle research: physicochemical properties of extremely small colloidal metal and semiconductor particles," *Chemical Reviews*, vol. 89, no. 8, pp. 1861–1873, 1989.

[2] R. Chapman and P. Mulvaney, "Electro-optical shifts in silver nanoparticle films," *Chemical Physics Letters*, vol. 349, no. 5-6, pp. 358–362, 2001.

[3] L. N. Lewis, "Chemical catalysis by colloids and clusters," *Chemical Reviews*, vol. 93, no. 8, pp. 2693–2730, 1993.

[4] A. Kiesow, J. E. Morris, C. Radehaus, and A. Heilmann, "Switching behavior of plasma polymer films containing silver nanoparticles," *Journal of Applied Physics*, vol. 94, no. 10, pp. 6988–6990, 2003.

[5] Y. Min, M. Akbulut, K. Kristiansen, Y. Golan, and J. Israelachvili, "The role of interparticle and external forces in nanoparticle assembly," *Nature Materials*, vol. 7, no. 7, pp. 527–538, 2008.

[6] J. L. Elechiguerra, J. L. Burt, J. R. Morones et al., "Interaction of silver nanoparticles with HIV-1," *Journal of Nanobiotechnology*, vol. 3, article 6, 2005.

[7] A. L. Stepanov, V. N. Popok, I. B. Khaibullin, and U. Kreibig, "Optical properties of polymethylmethacrilate with implanted silver nanoparticles," *Nuclear Instruments and Methods in Physics Research, Section B*, vol. 191, no. 1–4, pp. 473–477, 2002.

[8] Y. Badr and M. A. Mahmoud, "Enhancement of the optical properties of poly vinyl alcohol by doping with Silver nanoparticles," *Journal of Applied Polymer Science*, vol. 99, no. 6, pp. 3608–3614, 2006.

[9] P. C. Lebaron, Z. Wang, and T. J. Pinnavaia, "Polymer-layered silicate nanocomposites: an overview," *Applied Clay Science*, vol. 15, no. 1-2, pp. 11–29, 1999.

[10] J. M. Yeh, S. J. Liou, C. Y. Lin, C. Y. Cheng, Y. W. Chang, and K. R. Lee, "Anticorrosively enhanced PMMA-clay nanocomposite materials with quaternary alkylphosphonium salt as an intercalating agent," *Chemistry of Materials*, vol. 14, no. 1, pp. 154–161, 2002.

[11] T. H. Kim, L. W. Jang, D. C. Lee, H. J. Choi, and M. S. John, "Synthesis and rheology of intercalated polystyrene/Na^+-Montmorillonite nanocomposites," *Macromolecular Rapid Communications*, vol. 23, no. 3, pp. 191–195, 2002.

[12] Y. J. Lee and W. S. Lyoo, "Preparation of Atactic poly(vinyl alcohol)/silver composite nanofibers by electrospinning and their characterization," *Journal of Applied Polymer Science*, vol. 115, no. 5, pp. 2883–2891, 2010.

[13] V. K. Sharma, R. A. Yngard, and Y. Lin, "Silver nanoparticles: green synthesis and their antimicrobial activities," *Advances in Colloid and Interface Science*, vol. 145, no. 1-2, pp. 83–96, 2009.

[14] K. H. Hong, J. L. Park, I. N. Hwan Sul, J. H. Youk, and T. J. Kang, "Preparation of antimicrobial poly(vinyl alcohol) nanofibers containing silver nanoparticles," *Journal of Polymer Science, Part B*, vol. 44, no. 17, pp. 2468–2474, 2006.

[15] Z. H. Mbhele, M. G. Salemane, C. G. C. E. van Sittert, J. M. Nedeljković, V. Djoković, and A. S. Luyt, "Fabrication and characterization of silver-polyvinyl alcohol nanocomposites," *Chemistry of Materials*, vol. 15, no. 26, pp. 5019–5024, 2003.

[16] S. Mahendia, A. K. Tomar, and S. Kumar, "Electrical conductivity and dielectric spectroscopic studies of PVA-Ag nanocomposite films," *Journal of Alloys and Compounds*, vol. 508, no. 2, pp. 406–411, 2010.

[17] W. Brostow, R. Chiu, I. M. Kalogeras, and A. Vassilikou-Dova, "Prediction of glass transition temperatures: binary blends and copolymers," *Materials Letters*, vol. 62, no. 17-18, pp. 3152–3155, 2008.

[18] N. R. Jadhav, V. L. Gaikwad, K. J. Nair, and H. M. Kadam, "Glass transition temperature: basics and application in pharmaceutical sector," *Asian Journal of Pharmaceutics*, vol. 3, no. 2, pp. 82–89, 2009.

[19] J. B. González-Campos, Z. Y. García-Carvajal, E. Prokhorov et al., "Revisiting thermal relaxations of poly(vinyl alcohol)," *Journal of Applied Polymer Science*, vol. 125, pp. 4082–4090, 2012.

[20] J. B. Gonzalez-Campos, E. Prokhorov, G. Luna-Bárcenas et al., "Relaxations in chitin: evidence for a glass transition," *Journal of Polymer Science, Part B*, vol. 47, no. 9, pp. 932–943, 2009.

[21] J. B. Gonzalez-Campos, E. Prokhorov, G. Luna-Bárcenas, A. Fonseca-García, and I. C. Sanchez, "Dielectric relaxations of chitosan: the effect of water on the α-relaxation and the glass transition temperature," *Journal of Polymer Science, Part B*, vol. 47, no. 22, pp. 2259–2271, 2009.

[22] J. B. Gonzalez-Campos, E. Prokhorov, G. Luna-Bárcenas et al., "Chitosan/silver nanoparticles composite: molecular relaxations investigation by dynamic mechanical analysis and impedance spectroscopy," *Journal of Polymer Science, Part B*, vol. 48, no. 7, pp. 739–748, 2010.

[23] P. B. Bhargav, B. A. Sarada, A. K. Sharma, and V. V. R. N. Rao, "Electrical conduction and dielectric relaxation phenomena of PVA based polymer electrolyte films," *Journal of Macromolecular Science, Part A*, vol. 47, no. 2, pp. 131–137, 2010.

[24] A. L. Lee and A. J. Wand, "Microscopic origins of entropy, heat capacity and the glass transition in proteins," *Nature*, vol. 411, no. 6836, pp. 501–504, 2001.

[25] T. A. Hanafy, "Dielectric relaxation and alternating-current conductivity of gadolinium-doped poly(vinyl alcohol)," *Journal of Applied Polymer Science*, vol. 108, no. 4, pp. 2540–2549, 2008.

[26] S. L. Agrawal and A. Awadhia, "DSC and conductivity studies on PVA based proton conducting gel electrolytes," *Bulletin of Material Science*, vol. 27, no. 6, pp. 523–527, 2004.

[27] A. Linares, A. Nogales, D. R. Rueda, and T. A. Ezquerra, "Molecular dynamics in PVDF/PVA blends as revealed by dielectric loss spectroscopy," *Journal of Polymer Science, Part B*, vol. 45, no. 13, pp. 1653–1661, 2007.

[28] M. Hema, S. Selvasekerapandian, and G. Hirankumar, "Vibrational and impedance spectroscopic analysis of poly(vinyl alcohol)-based solid polymer electrolytes," *Ionics*, vol. 13, no. 6, pp. 483–487, 2007.

[29] J. Zhang, M. Mine, D. Zhu, and M. Matsuo, "Electrical and dielectric behaviors and their origins in the three-dimensional polyvinyl alcohol/MWCNT composites with low percolation threshold," *Carbon*, vol. 47, no. 5, pp. 1311–1320, 2009.

[30] F. Garcia, A. Garcia-Bernabe, V. Compan, R. Diaz-Calleja, J. Guzman, and E. Riande, "Relaxation behavior of acrylate and methacrylate polymers containing dioxacyclopentane rings in the side chains," *Journal of Polymer Science B*, vol. 39, no. 3, pp. 286–299, 2001.

[31] V. Compan, J. Guzman, R. Diaz-Calleja, and E. Riande, *Relxation behavior of methacrylic polymers with bulky hydrophilic groups in their structuresJournal of Polymer Science B*, vol. 37, pp. 3027–3037, 1999.

[32] G. G. Raju, *Dielectrics in Electrical Fields*, Marcel Dekker, New York, NY, USA, 2003.

[33] A. Gautam and S. Ram, "Preparation and thermomechanicalproperties of Ag-PVA nanocomposite films," *Materials Chemistry and Physics*, vol. 119, no. 1-2, pp. 266–271, 2010.

[34] M. Köhler, P. Lunkenheimer, and A. Loidl, "Dielectric and conductivity relaxation in mixtures of glycerol with LiCl," *European Physical Journal E*, vol. 27, no. 2, pp. 115–122, 2008.

[35] M. D. Migahed, N. A. Bakr, M. I. Abdel-Hamid, O. El-Hanafy, and M. El-Nimr, "Dielectric relaxation and electric modulus behavior in poly(vinyl alcohol)-based composite systems," *Journal of Applied Polymer Science*, vol. 59, no. 4, pp. 655–662, 1996.

[36] K. P. Singh and P. N. Gupta, "Study of dielectric relaxation in polymer electrolytes," *European Polymer Journal*, vol. 34, no. 7, pp. 1023–1029, 1998.

[37] M. C. Hernández, N. Suárez, L. A. Martínez, J. L. Feijoo, S. Lo Mónaco, and N. Salazar, "Effects of nanoscale dispersion in the dielectric properties of poly(vinyl alcohol)-bentonite nanocomposites," *Physical Review E*, vol. 77, no. 5, Article ID 051801, 2008.

[38] N. F. Mott, *Metal-Insulator Transitions*, Taylor & Francis, London, UK, 1990.

[39] G. C. Psarras, "Hopping conductivity in polymer matrix-metal particles composites," *Composites Part A*, vol. 37, no. 10, pp. 1545–1553, 2006.

[40] S. Capaccioli, M. Lucchesi, P. A. Rolla, and G. Ruggeri, "Dielectric response analysis of a conducting polymer dominated by the hopping charge transport," *Journal of Physics Condensed Matter*, vol. 10, no. 25, pp. 5595–5617, 1998.

[41] H. Tian and H. Tagaya, "Dynamic mechanical property and photochemical stability of perlite/PVA and OMMT/PVA nanocomposites," *Journal of Materials Science*, vol. 43, no. 2, pp. 766–770, 2008.

[42] C. C. Yang, Y. J. Lee, and J. M. Yang, "Direct methanol fuel cell (DMFC) based on PVA/MMT composite polymer membranes," *Journal of Power Sources*, vol. 188, no. 1, pp. 30–37, 2009.